Fundamental Analysis of a Digital Spiking Neuron for Its Spike-Based Coding

Hiroyuki Torikai

Graduate School of Engineering Science, Osaka University
torikai@sys.es.osaka-u.ac.jp

Abstract. A *digital spiking neuron* (DSN) is a wired system of shift registers. By adjusting the parameters (e.g., number of registers and wiring pattern), the DSN can generate spike-trains having various inter-spike-intervals. In this paper we present some basic relations between parameters of the DSN and characteristics of the spike-train. We also discuss that the presented results will be fundamental to consider ISI-based coding abilities of the DSN.

1 Introduction

Various simplified spiking neuron models have been proposed and their dynamics have been investigated intensively (see [1]-[8] and references therein). Using such spiking neuron models, pulse-coupled neural networks (PCNNs) have been constructed and their possible functions and application potentials have been investigated, e.g., image processing based on synchronization of spike-trains [6]-[8]. Inspired by such spiking neuron models, we have proposed a *digital spiking neuron* (DSN) [9][10] as shown in Fig.1. Depending on parameters (i.e., number of registers and wiring pattern among the registers), the DSN can generate spike-trains with various patterns of inter-spike-intervals. One of the biggest motivations for considering the DSN is that the parameters of the DSN can be dynamically adjusted in real electrical circuits such as *field programmable gate array* (FPGA). This means that DSN is suitable for on-chip learning. It should be note that it is troublesome to realize dynamical parameter adjustment (e.g., conductance and nonlinearity) of spiking neurons that are implemented in analog integrated circuits. Previous results on the DSN include the followings.

(a) A learning algorithm for the DSN was proposed in order to approximate spike-trains generated by analog neuron models [11]. The results suggest that the DSN may be able to approximate dynamics of neuron models as well as biological neurons. Hence the results may contribute to develop communication interface with biological neurons, e.g., a digital circuitry that can mimic spike-based communication protocols of neurons.

(b) Another learning algorithm for the DSN was proposed in order to generate spike-trains whose characteristics are suitable for ultra-wide band (UWB) impulse-radio technologies [10]. The results may contribute to develop a bio-inspired spike-based engineering system, e.g., UWB sensor network with bio-inspired learning abilities.

(c) Some spike-based coding abilities of the DSN have been clarified [9][12]. Also, a PCNN of DSNs has been constructed and its application potentials (e.g., spike-based multiplex communication) have been studied.

M. Ishikawa et al. (Eds.): ICONIP 2007, Part II, LNCS 4985, pp. 87–96, 2008.

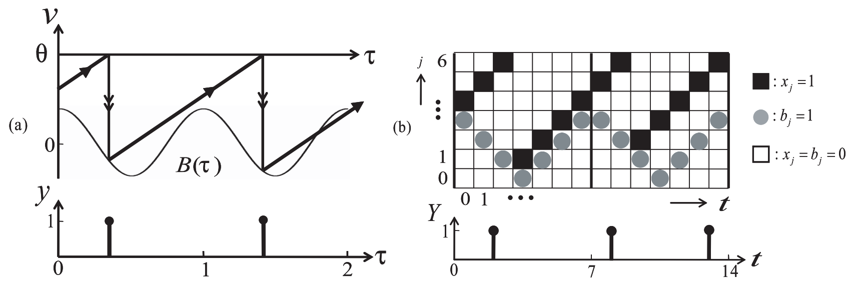

Fig. 1. (a) Analog spiking neuron model. Integrate-and-fire behavior of analog potential v for continuous-time τ [1]-[4]. (b) Digital spiking neuron. Shift-and-reset behavior of digital state x_j for discrete-time t [9][10].

In this paper we present some basic relations between parameters of the DSN and characteristics of the spike-train. Such results have not been shown in the previous works. We also discuss that the presented results will be fundamentals to develop applications of the DSN such as the spike-based coding.

2 Digital Spiking Neuron

In this section we introduce our *digital spiking neuron* (DSN) proposed in Refs. [9][10]. The DSN operates on a discrete time $t = 0, 1, 2, \cdots$. Fig.2(a) shows the DSN. First, let us consider the p-cells that are usual shift registers. Let the number of p-cells be denoted by M, where $M \geq 1$. Let $i \in \{0, 1, \cdots, M-1\}$ be an index for the p-cell. The p-cell has a digital state $p_i \in \{0, 1\} \equiv \boldsymbol{B}$, where "$\equiv$" denotes "*definition*" throughout this paper. The p-cells are ring-coupled and their dynamics is described by

$$p_i(t+1) = p_{i+1 \ (\mathrm{mod} M)}(t). \tag{1}$$

For convenience, initial states of the p-cells are fixed as follows: $p_i(0) = 1$ for $i = Int(\frac{M-1}{2})$, and $p_i(0) = 1$ otherwise, where $Int(\alpha)$ gives the integer part of α. Then the p-cells oscillate periodically with period M. In order to consider dynamics of the DSN, we introduce a state vector $\boldsymbol{P}(t) \equiv (p_0(t), \cdots, p_{M-1}(t))^t \in \boldsymbol{B}^M$. Second, let us consider the reconfigurable wirings from p-cells to x-cells. Let the number of x-cells be denoted by N, where $N \geq M$. Let $j \in \{0, 1, \cdots, N-1\}$ be an index for the x-cell. In the dotted box of Fig.2(a), the left terminals are denoted by $\{p_0, \cdots, p_i, \cdots, p_{M-1}\}$ and the right terminals are denoted by $\{b_0, \cdots, b_j, \cdots, b_{N-1}\}$. Each left terminal p_i has one wiring and each right terminal b_j can accept any number of wirings. In order to describe pattern of the wirings, let us define an $N \times M$ matrix $\boldsymbol{A}$ whose elements are $a(j, i) = 1$ if p_i is wired to b_j, and $a(j, i) = 0$ otherwise. The matrix $\boldsymbol{A}$ is referred to as a *wiring matrix*. In the case of Fig.2(a), the wiring matrix is given by $a(i, i) = 1$ for all i and $a(i, j) = 0$ for $i \neq j$. The right N terminals output a signal vector $(b_0(t), b_1(t), \cdots, b_{N-1}(t))^t \equiv \boldsymbol{b}(t) \in \boldsymbol{B}^N$ which is given by

$$\boldsymbol{b}(t) = \boldsymbol{A}\boldsymbol{P}(t). \tag{2}$$

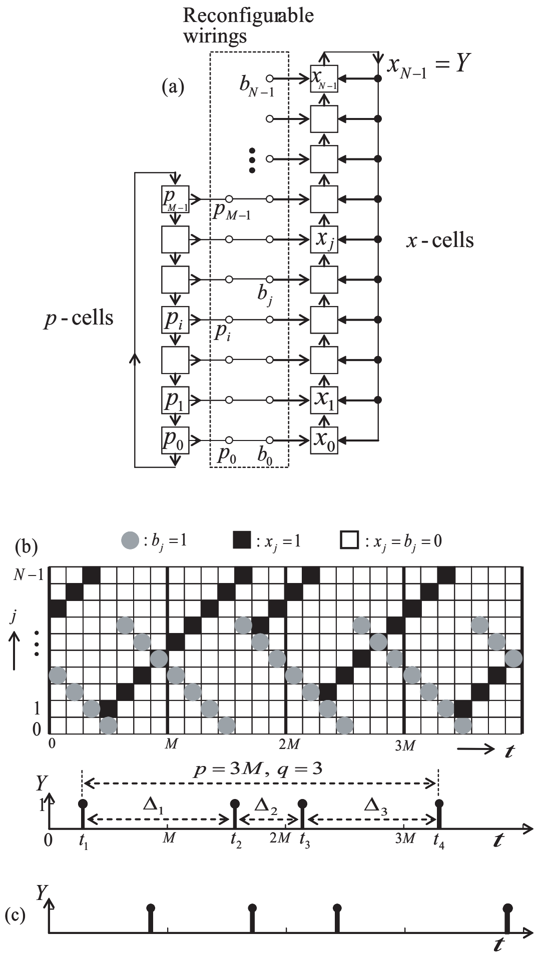

Fig. 2. (a) Digital spiking neuron. $M = 7$ and $N = 10$. (b) Basic dynamics. The initial state is $x_7(0) = 1$. p is the period and q is the ISI-number. (c) Co-existing spike-train. The initial state is $x_3(0) = 1$.

The signal $\boldsymbol{b}(t)$ is referred to as a *base signal* and is to be periodic with period M as illustrated by gray circles in Fig.2(b). Third, let us consider the x-cells that are specialized shift registers. Each x-cell has a digital state $x_j \in \boldsymbol{B}$. The x-cell has three digital inputs (b_j, x_{N-1}, x_{j-1}) for $j \geq 1$ and has two digital inputs (b_j, x_{N-1}) for $j = 0$. If $x_{N-1}(t) = 0$, the x-cell operates $x_j(t+1) = x_{j-1}(t)$ for $j \geq 1$ and operates $x_j(t+1) = 0$ for $j = 0$. If $x_{N-1}(t) = 1$, the x-cell operates $x_j(t+1) = b_j(t)$ for all j. Let us define a state vector of the x-cells: $(x_0(t), \cdots, x_{N-1}(t))^t \equiv \boldsymbol{X}(t) \in \boldsymbol{B}^N$. Then, using a shift operator $\mathcal{S}((x_0, \cdots, x_{N-1})^t) = (0, x_0, \cdots, x_{N-2})^t$, the dynamics of the x-cells is described by

$$\boldsymbol{X}(t+1) = \begin{cases} \mathcal{S}(\boldsymbol{X}(t)) & \text{if } x_{N-1}(t) = 0 \text{ (Shift)}, \\ \boldsymbol{b}(t) & \text{if } x_{N-1}(t) = 1 \text{ (Reset)}. \end{cases} \tag{3}$$

Basic dynamics of the x-cells is illustrated by black boxes in Fig.2(b). If $x_{N-1} = 0$, the DSN is governed by the *shift operation*: the state $x_j = 1$ is shifted upward. At $t = t_1$, the $(N-1)$-th x-cell has state $x_{N-1} = 1$. In this case the DSN is governed by the *reset operation*: the state vector $\boldsymbol{X}$ is reset to $\boldsymbol{X}(t_1+1) = \boldsymbol{b}(t_1) = (0, 1, 0, \cdots, 0)^t$. Repeating such *shift-and-reset behavior*, the x-cells oscillate as shown in Fig.2(b). The state x_{N-1} of the $(N-1)$-th x-cell is used as an output Y of the DSN. Then the DSN outputs a discrete-time spike-train $Y(t)$ as shown in Fig.2(b):

$$Y(t) \equiv x_{N-1}(t) \in \boldsymbol{B}, \quad t = 0, 1, 2, \cdots. \tag{4}$$

As a result the DSN is governed by the set of Equations (1), (2), (3) and (4). Also, the DSN is characterized by the following parameters:

of p-cells M, # of x-cells N, elements $a(j, i)$ of wiring matrix $\boldsymbol{A}$

where "#" denotes "*the numbers*." The DSN has a controllable initial state vector $\boldsymbol{X}(0) = (x_0(0), x_1(0), \cdots, x_{N-1}(0))^t$ of the x-cells. In this paper we assume that only one element of $\boldsymbol{X}(0)$ is 1. The black boxes in Fig.2(b) show a trajectory of $\boldsymbol{X}$ under such an assumption. As shown in Fig.2(b), let $t_n \in \{0, 1, 2, \cdots, \}$, $n = 1, 2, 3, \cdots$ be the n-th spike position. Also let $\Delta_n = t_{n+1} - t_n$ be the n-th *inter-spike-interval* (ISI). Here let us give some definitions.

Definition 1. A spike-train Y_* is said to be a *periodic spike-train* if there exist positive integers p and q such that $t_{n+q} = t_n + p$ for all $n \geq 1$. In this case, the possible minimum integers p and q are said to be *period* and *ISI-number* of the periodic spike-train Y_*. q means the number of ISI-intervals during the period $0 \leq t \leq p$, and the period is to be $p = \sum_{n=1}^{q} \Delta_n$. A spike position t_* of a periodic spike-train Y_* is said to be a *periodic spike position*. A spike position $t_1 = t_e$ is said to be an *eventually periodic spike position* if t_e is not a periodic spike position but t_n is a periodic spike position for some $n \geq 2$.

The spike-train $Y(t)$ in Fig.2(b) is a periodic spike-train with period $p = 3M$ and ISI-number $q = 3$, where $M = 7$. The DSN can exhibit the following phenomena.

- The DSN has the finite states $\boldsymbol{P}$ and $\boldsymbol{X}$ operating on the discrete-time t. Then the DSN oscillates periodically and generates a periodic spike-train Y_* in a steady state. The periodic spike-train Y_* can have various patterns of ISIs $(\Delta_1, \Delta_2, \cdots, \Delta_q)$.
- The periodic spike-trains $Y(t)$ in Fig.2(b) and (c) are caused by different initial states $x_7(0) = 1$ and $x_3(0) = 1$, respectively. Such phenomenon is referred to as *co-existence for initial state*. The DSN can have multiple co-existing periodic spike-trains and generates one of them depending on the initial state $\boldsymbol{X}(0)$.
- The DSN may have an eventually periodic spike position depending on parameter values. The existence of an eventually periodic spike position implies existence of a transient phenomenon.

3 Analysis of Various Spike-Trains

In order to consider dynamics of the spike position t_n, let us define the following *base index function* $\beta(t) \equiv j$ such that $b_j(t) = 1$. Fig.3(a) shows the base index function $\beta(t)$

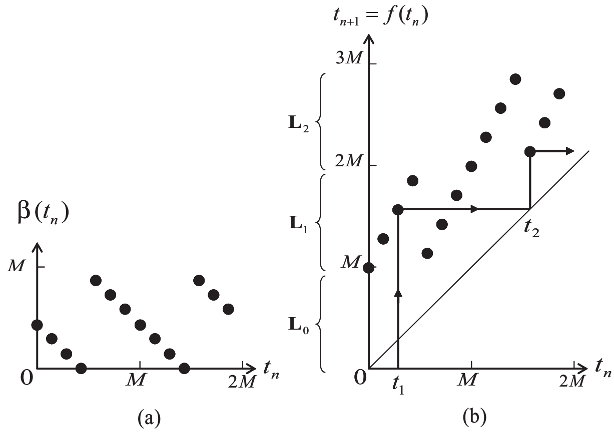

Fig. 3. Maps corresponding to the DSN in Fig.2(a). (a) Base index function $\beta(t)$. (b) Spike position map f.

corresponding to the DSN in Fig.2(a). The base index function $\beta(t)$ can be regarded as a trajectory of the gray circle (i.e., the state "$b_j(t) = 1$") in Fig.2(b). The shape of $\beta(t)$ is determined by the wiring matrix $\boldsymbol{A}$ as follows:

$$\beta(t) = j \ \text{ such that } \ a(j, M + \gamma - t \ (\text{mod} M)) = 1 \quad \text{for } 0 \leq t \leq M-1 \tag{5}$$

where $\beta(t+M) = \beta(t)$. Using the base index function $\beta(t)$, the dynamics of the spike position t_n is described by the following *spike position map*:

$$t_{n+1} = f(t_n) \equiv t_n + N - \beta(t_n), \quad f : \boldsymbol{L} \to \boldsymbol{L} \equiv \{0, 1, 2, \cdots\}. \tag{6}$$

Fig.3(b) shows the spike position map f corresponding to the DSN in Fig.2(a). The first spike position t_1 of the spike position map f is determined by the initial state of the x-cells as follows:

$$t_1 = j \ \text{ such that } \ x_{N-1-j}(0) = 1. \tag{7}$$

We emphasize that the shape of the spike position map f is determined by the wiring matrix $\boldsymbol{A}$ which describes pattern of the reconfigurable wirings of the DSN (see Fig.2(a)). That is, various shapes of f (i.e., various dynamics of the spike position t_n) can be realized by adjusting the wiring matrix $\boldsymbol{A}$. In the following part, we give some new results by focusing on a simple form of $\boldsymbol{A}$.

Let us focus on the following parameter case hereafter:

$$M \geq 1, \quad N = Int(\tfrac{3M-1}{2}), \quad a(j,i) = \begin{cases} 1 \text{ for } \ i = j, \\ 0 \text{ otherwise.} \end{cases} \tag{8}$$

In this case the DSN is characterized by one parameter: the number M of the p-cells. For short, let us refer to M as a *system size* hereafter. The DSN in Fig.2(a) satisfies the condition in Equation (8) with the system size $M = 7$. We can see in Fig.2(a) that

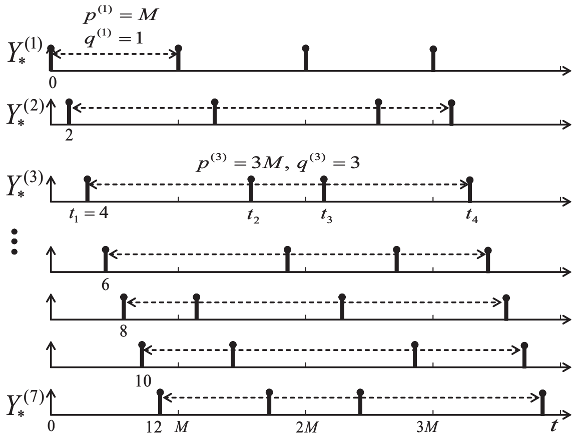

Fig. 4. The co-existing periodic spike-trains under the parameter condition in Equation (8) with the system size $M = 14$. The number S of co-existing periodic spike-trains is 7.

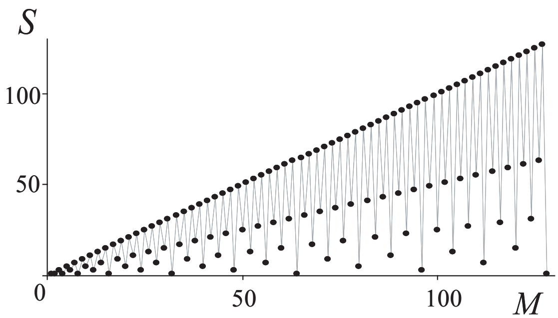

Fig. 5. Characteristics of the number S of co-existing periodic spike-trains

the pattern of wirings is simple: each right terminal p_i is wired to each left terminal b_i straightly. Under the condition in Equation (8), the spike position map f is given by

$$f(t_n) = \begin{cases} 2t_n + M & \text{for } \ 0 \leq t_n \leq \gamma, \\ 2t_n & \text{for } \ \gamma + 1 \leq t_n \leq M - 1, \end{cases} \qquad f(t_n + M) = f(t_n) + M. \quad (9)$$

Fig.3(b) shows this spike position map f for $M = 7$. As shown in this figure, let us define the sets $\boldsymbol{L}_k \equiv \{kM,\ kM+1,\ kM+2,\ \cdots,\ kM+M-1\}$, where $k = 0, 1, 2, \cdots$. Then we can confirm $f(\boldsymbol{L}_k) \subseteq \boldsymbol{L}_{k+1}$, where $f(\boldsymbol{L}_k)$ represents the set $\{f(t) \mid t \in \boldsymbol{L}_k\}$ of images of f. This means that the spike-train $Y(t)$ has one spike in each set $\boldsymbol{L}_k$, i.e.,

$$t_n \in \boldsymbol{L}_{n-1} \quad \text{for all} \quad n = 1, 2, 3, \cdots. \quad (10)$$

From Equation (10), we can restrict the following first spike position into $t_1 \in \boldsymbol{L}_0$. Let us refer to $\boldsymbol{L}_0$ as an *initial state set*. In addition, from Equation (10), we can have the relation $p = Mq$. In the case of Fig.2(b), we can confirm $q = 3$ and $p = 3M$.

3.1 Number of Periodic Spike-Trains

Fig.4 shows all the co-existing periodic spike-trains of the DSN for the system size $M = 14$. Let us consider the following quantity:

$$S \equiv \# \text{ of co-existing periodic spike-trains for the initial state } \boldsymbol{X}(0).$$

In the case of Fig.4, $S = 7$. Fig.5 shows characteristics of S for the system size M, that can be given by a function of M as shown below. Let M_0 be the maximum odd divisor of M and let M be decomposed into even and odd components:

$$M = 2^r M_0, \quad r \in \{0, 1, 2, \cdots\}, \quad M_0 \in \{1, 3, 5, \cdots\}. \tag{11}$$

In the case of Fig.4, $M_0 = 7$ and $r = 1$. Let us divide the initial state set $\boldsymbol{L}_0$ into the following two disjoint subsets $\boldsymbol{L}_p$ and $\boldsymbol{L}_e$:

$$\boldsymbol{L}_p \equiv \{0,\ \ 2^r,\ \ 2^r 2,\ \ \cdots,\ \ 2^r(M_0 - 1)\}, \qquad \boldsymbol{L}_e \equiv \boldsymbol{L}_0 - \boldsymbol{L}_p. \tag{12}$$

In the case of Fig.4, $\boldsymbol{L}_p = \{0, 2, \cdots, 12\}$ and $\boldsymbol{L}_e = \{1, 3, \cdots, 13\}$. We can generalize this results into the following properties for any given system size M.

- The number S of co-existing periodic spike-trains is M_0.
- $\boldsymbol{L}_p$ is a set of all the periodic spike positions in the initial state set $\boldsymbol{L}_0$.
- $\boldsymbol{L}_e$ is a set of all the eventually periodic spike positions in $\boldsymbol{L}_0$.

Proof of these properties will be given in a journal paper.

3.2 Period and ISI-Number

Here let us consider periods and ISI-numbers of the co-existing spike-trains. Let us give some definitions (see Fig.4).

Definition 2. Let the S pieces of co-existing periodic spike-trains be denoted by $\{Y_*^{(1)}, Y_*^{(2)}, \cdots, Y_*^{(S)}\}$ in the order of the first spike position t_1. Let the period and the ISI-number of each spike-train $Y_*^{(s)}$ be denoted by $p^{(s)}$ and $q^{(s)}$, respectively, where $s \in \{1, 2, \cdots, S\}$. Let the least common multiple of the periods $\{p^{(s)}\}$ be denoted by P and let it be referred to as a *common period*. Let the least common multiple of the ISI-numbers $\{q^{(s)}\}$ be denoted by Q and let it be referred to as a *common ISI-number*.

The set $\{Y_*^{(s)}\}$ of co-existing periodic spike-trains can be characterized by the common period P and the common ISI-number Q. In the case of Fig.4, the common period is $P = 3M$ and the common ISI-number is $Q = 3$. Fig.6 shows characteristics of Q for the system size M, that can be given by a function of M as shown below. As a preparation, let us define the following function $K(l)$ for a positive odd integer l:

$$K(l) \equiv \min\{z \mid z \in \{1, 2, \cdots, l\},\ 2^z - 1 \pmod{l} = 0\}. \tag{13}$$

For example $K(7) = 3$. Let the system size M be given. Let a periodic spike position $t_1 \in \boldsymbol{L}_p$ be the first spike position of a periodic spike-train $Y_*^{(s)}$. Let a fraction $\frac{t_1}{M}$ be reduced into an irreducible fraction $\frac{m'}{M'}$. Then we can give the following properties.

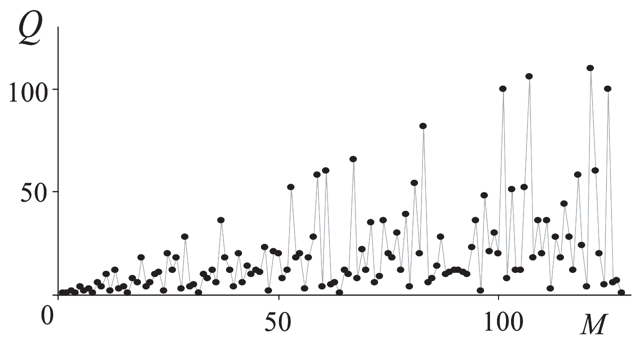

Fig. 6. Characteristics of the common ISI-number Q

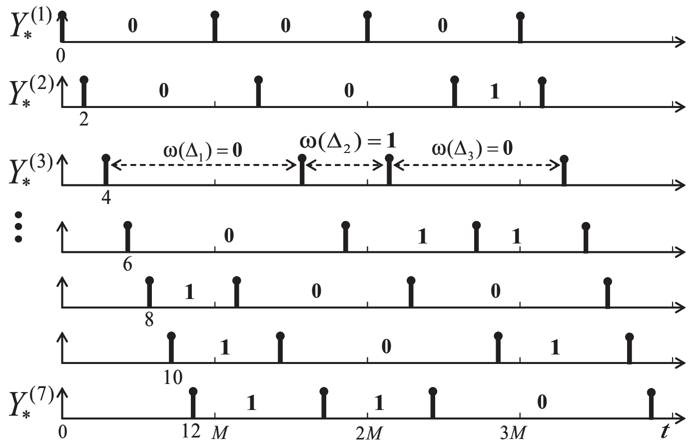

Fig. 7. ISI coding. The parameters satisfy the condition in Equation (8) with the system size $M = 14$. The spike-trains are identical with that in Fig.4. The periodic spike-trains have one-to-one relation to all the 3-bit binary numbers except for $(1, 1, 1)$.

- The period $p^{(s)}$ and the ISI-number $q^{(s)}$ of the spike-train $Y_*^{(s)}$ are given by $MK(M')$ and $K(M')$, respectively.
- The common period P and the common ISI-number Q of the co-existing periodic spike-trains $\{Y_*^{(s)}\}$ are given by $MK(M_0)$ and $K(M_0)$, respectively.

Proof of these properties will be given in a journal paper. In the case of Fig.4, $Y_*^{(1)}$ has the first spike position $t_1 = 0$. The fraction $\frac{0}{14}$ can be reduced into an irreducible fraction $\frac{0}{1}$ and then $Y_*^{(1)}$ has period $p^{(1)} = MK(1) = M$ and ISI-number $q^{(1)} = K(1) = 1$. $Y_*^{(3)}$ has the first spike position $t_1 = 4$. The fraction $\frac{4}{14}$ can reduced into an irreducible fraction $\frac{2}{7}$ and then $Y_*^{(3)}$ has period $p^{(3)} = MK(7) = 3M$ and ISI-number $q^{(3)} = K(7) = 3$. The common period and the common ISI-number can be given by $P = MK(7) = 3M$ and $Q = K(7) = 3$, respectively.

3.3 Inter-Spike-Interval Coding

Fig.7 shows the co-existing periodic spike-trains for the system size $M = 14$. As shown in this figure, let us consider an ISI coding:

$$\omega(\Delta_n) = 0 \ \text{for} \ \Delta_n \geq M, \qquad \omega(\Delta_n) = 1 \ \text{for} \ \Delta_n \leq M - 1. \tag{14}$$

Using the ISI coding, the periodic spike-train $Y_*^{(3)}$ in Fig.7 is coded by a 3-bit digital sequence $(\omega(\Delta_1), \omega(\Delta_2), \omega(\Delta_3)) = (0, 1, 0)$. We refer to this sequence as a *ISI code*. In the case of Fig.7, the common ISI-number is $Q = 3$ and each spike-train $Y^{(s)}$ is coded by a 3-bit ISI code. We can see that the set $\{Y_*^{(s)}\}$ of co-existing periodic spike-trains can have one-to-one relation to the set of 3-bit binary numbers except for $(1, 1, 1)$. For general system size M, recalling Theorem 2, the common ISI-number is to be $Q = K(M_0)$. In this case the co-existing periodic spike-trains are coded by Q-bit ISI codes $(\omega(\Delta_1), \omega(\Delta_2), \cdots, \omega(\Delta_Q))$. We can give the following property for a given system size M.

- Let M be given. A periodic spike-train $Y_*^{(s)}$ having a first spike position $t_1 \in \boldsymbol{L}_p$ is coded by a Q-bit ISI code $(\omega(\Delta_1), \omega(\Delta_2), \cdots, \omega(\Delta_Q))$ such that

$$\textstyle\sum_{n=1}^{Q} 2^{Q-n} \omega(\Delta_n) = \frac{2^Q - 1}{M} t_1. \tag{15}$$

Proof of this property will be given in a journal paper. Equation (15) suggests that the set of co-existing periodic spike-trains can have one-to-one relation to a set of some Q-bit binary numbers, where the binary number representation of $\frac{2^Q-1}{M}t_1$ is identical with the ISI code $(\omega(\Delta_1), \omega(\Delta_2), \cdots, \omega(\Delta_Q))$. In the case of $Y_*^{(3)}$ in Fig.7, we can confirm that the binary number representation of $\frac{2^Q-1}{M}t_1 = \frac{7}{14}4 = 2$ is $(0, 1, 0)$ which is identical with the ISI code.

Discussion: Ref. [9] proposes a pulse-coupled network of DSNs and its application to a multiplex communication system, where the DSN is used to code binary information into spike-train. The theorems in this paper will be mathematical basis to investigate such an application as follows.

(i) The number S of co-existing periodic spike-trains corresponds to the number of binary numbers (informations) that can be coded into the spike-train.

(ii) The common ISI-number Q corresponds to the code length.

(iii) Equations (7) and (15) show relation between the initial state $\boldsymbol{X}(0)$ and the ISI code. These equations suggest that the DSN can code a binary number (information) into the spike-train by adjusting the initial state (which can be regarded as an input) appropriately.

We note that Ref. [9] analyzes the DSN for a very limited parameter case, and this paper generalizes the analysis.

4 Conclusions

We have introduced the *digital spiking neuron* (DSN) and clarified the basic relations between parameter of the DSN and characteristics of the spike-train, e.g., the number of co-existing periodic spike-trains, their initial states, their periods, and their ISI-numbers. We have also clarified the relation between the initial state of the spike-train and its corresponding ISI code, and have shown that the set of co-existing periodic spike-trains can have one-to-one relation to a set of some binary numbers. Then we have discussed that the presented results will be fundamental to study coding functions of the DSN. Future problems include: (a) analysis of the DSN for various cases of wiring matrix; (b) synthesis of a pulse-coupled neural network of DSNs with interesting functions; and (c) development of on-chip learning algorithms for the DSN and/or its pulse-coupled neural network.

Acknowledgement

The author would like to thank Professor Kazuyuki Aihara of Tokyo Univ. and Professor Masato Okada of Tokyo Univ. for valuable discussions. The author would like to thank Professor Toshimitsu Ushio of Osaka Univ. and Professor Toshimichi Saito of Hosei Univ. for valuable advises.

References

1. Perez, R., Glass, L.: Bistability, period doubling bifurcations and chaos in a periodically forced oscillator. Phys. Lett. 90A(9), 441–443 (1982)
2. Izhikevich, E.M.: Dynamical systems in neuroscience. MIT Press, Cambridge (2006)
3. Torikai, H., Saito, T.: Synchronization phenomena in pulse-coupled networks driven by spike-train inputs. IEEE Trans. Neural Networks 15(2), 337–347 (2004)
4. Lee, G., Farhat, N.H.: The bifurcating neuron network 2. Neural networks 15, 69–84 (2002)
5. Eckhorn, R.: Neural mechanisms of scene segmentation: recordings from the visual cortex suggest basic circuits for linking field models. IEEE Trans. Neural Networks 10(3), 464–479 (1999)
6. Hopfield, J.J., Herz, A.V.M.: Rapid local synchronization of action potentials: Toward computation with coupled integrate-and-fire neurons. Proc. Natl. Acad. Sci. USA 92, 6655–6662 (1995)
7. Campbell, S.R., Wang, D., Jayaprakash, C.: Synchrony and desynchrony in integrate-and-fire oscillators. Neural computation 11, 1595–1619 (1999)
8. Nakano, H., Saito, T.: Grouping synchronization in a pulse-coupled network of chaotic spiking oscillators. IEEE Trans. Neural Networks 15(5), 1018–1026 (2004)
9. Torikai, H., Hamanaka, H., Saito, T.: Reconfigurable Digital Spiking Neuron and its Pulse-Coupled Network: Basic Characteristics and Potential Applications. IEEE Trans. CAS-II 53(8), 734–738 (2006)
10. Torikai, H.: Basic Characteristics and Learning Potential of a Digital Spiking Neuron. IEICE Trans. Fundamentals (to appear, 2007)
11. Torikai, H., Funew, A., Saito, T.: Approximation of Spike-trains by Digital Spiking Neuron. In: Proc. of IJCNN, paper #1698 (2007)
12. Kabe, T., Torikai, H., Saito, T.: Synchronization via multiplex spike-trains in digital pulse-coupled networks. In: King, I., Wang, J., Chan, L.-W., Wang, D. (eds.) ICONIP 2006. LNCS, vol. 4234, pp. 1141–1149. Springer, Heidelberg (2006)